PERIODICO di MINERALOGIA
established in 1930

DIPARTIMENTO
DI SCIENZE DELLA TERRA

SAPIENZA
UNIVERSITÀ DI ROMA

An International Journal of
Mineralogy, Crystallography, Geochemistry,
Ore Deposits, Petrology, Volcanology
and applied topics on Environment, Archaeometry and Cultural Heritage

Mineralogy and genetic characteristics of the Rudnik Pb-Zn/Cu,Ag,Bi,W polymetallic deposit (Central Serbia) - New occurrence of Pb(Ag)Bi sulfosalts

Jovica N. Stojanović [a,*], Ana S. Radosavljević-Mihajlović [a], Slobodan A. Radosavljević [a], Nikola S. Vuković [b], Aleksandar M. Pačevski [c]

[a] Applied Mineralogy Unit, Institute for Technology of Nuclear and Other Mineral Raw Materials, Franchet d'Esperey 86, P.O. Box 390, 11000 Belgrade, Serbia
[b] Laboratory for Scanning Electron Microscopy, Faculty of Mining and Geology, University of Belgrade, Đušina 7, 11000 Belgrade, Serbia
[c] Department for Mineralogy and Petrology, Faculty of Mining and Geology, University of Belgrade, Đušina 7, 11000 Belgrade, Serbia

ARTICLE INFO

Submitted: August 2015
Accepted: March 2016
Available on line: April 2016

* Corresponding author:
j.stojanovic@itnms.ac.rs

DOI: 10.2451/2016PM605

How to cite this article:
Stojanović J.N. et al. (2016) Period. Mineral. 85, 121-135

ABSTRACT

Aschamalmite, ideally $Pb_{6-3x}Bi_{2+x}S_9$, ordered monoclinic homeotype of heyrovskýite from the Rudnik Pb-Zn/Cu,Ag,Bi,W polymetallic deposit in the central part of Serbia has been investigated. This polymetallic deposit includes over 90 hydrothermal and skarn-replacement orebody types, primarily hosted by Cretaceous sediments and occassionally by Oligocene dykes and sills of dacitic composition, and contact-metamorphic-metasomatic rocks. These rocks are host to an assemblage of pyrrhotite, colloform pyrite, chalcopyrite, galena, arsenopyrite, native bismuth and scheelite as well as minor pyrite, sphalerite, bismuthinite, argentopentlandite, and native silver. The chemical composition of the ore is very complex, where weight contents of valuable metals range as follows (%): Zn 0.49-4.49; Pb 0.90-5.66; Cu 0.08-2.18; WO_3 0.05-1.18; Ag 0.005-0.030; Bi 0.005-0.081; and Cd 0.002-0.016. Well-developed aschamalmite crystals have not been observed, only stocky and spindle-like aggregates up to 10 mm in length intergrown with sulfides. Electron-microprobe analysis gave the average crystallochemical formula $(Pb_{5.82}Ag_{0.20})_{\Sigma 6.02}Bi_{2.03}(S_{8.93}Te_{0.02}Se_{0.01})_{\Sigma 8.96}$. The strongest diffraction reflections of the X-ray powder diffraction pattern [d(in Å)(I)] are: 3.419(100), 3.382(92), and 3.334(66). Monoclinic unit-cell parameters are a=13.727(7); b=4.122(3); c=31.32(2)Å; β=90.72(5) °; and V=1771.8(1)Å^3. Mineral assemblages and genesis of the Rudnik polymetallic deposit are discussed in detail and the thiobismuthite mineralization has been compared with similar well-known deposits.

Keywords: Ag-bearing aschamalmite; thiobismuthites; argentopentlandite; Pb-Zn/Cu,Ag,Bi,W polymetallic ore; Rudnik; Central Serbia.

INTRODUCTION

Thiobismuthite minerals belonging to the AgS_2-Bi_2S_3-PbS system were studied by several investigators (e.g. Wernick, 1960; Craig, 1967; Hoda et al., 1975; Makovicky, 1977; Makovicky and Karup-Møller, 1977 a,b; Mozgova, 1985; Wu, 1987; Chang et al., 1988; Wang, 1999; Biruk and Skakun, 2000; Chutas et al., 2008; Voudouris et al., 2013). Crystal structures of thiobismuthites are based on the structure of galena. Structural closeness, similarity of chemical composition, optical and other physical properties all created difficulties in determination of mineral species within this group. Moreover, the reflectance curves of all sulfosalts within this group are located close to galena and bismuthinite reflectance spectra (Godovikov, 1972; Ramdohr, 1980; Ciobanu et al., 2004).

Moëlo et al. (2008) summarized the status of Bi-

sulfosalt minerals in the same system. Aschamalmite has a chemical composition close to that of heyrovskýite ($Pb_6Bi_2S_9$), but shows a different crystal structure. The general formula for aschamalmite is $Pb_6Bi_2S_9$, with a Bi/Pb atomic ratio of ⅓. It was described for the first time by Mumme et al. (1983), who found the mineral in a leucocratic albite-gneiss from Ascham Alm in the Untersulzbach Valley in Austria. Aschamalmite was associated with several other sulfates and sulfosalts, and sulfides such as pyrrhotite, chalcopyrite, pyrite, galena, galenobismutite and friedrichite. It is closely related to heyrovskýite and several natural and synthetic phases in the Bi_2S_3-PbS system. Mumme et al. (1983) suggested that aschamalmite was not a dimorph of heyrovskýite in the strict sense because the latter always contained a significant amount of Ag and a corresponding extra Bi (Bi>2 atoms per formula unit, apfu) for charge balance. However, Ag-free heyrovskýite was subsequently found at Vulcano, Aeolian Islands, Italy (Callegari and Boiocchi, 2009; Borodaev et al., 2003; Pinto et al., 2011). Aschamalmite was also determined in USA [Granite Gap, Hidalgo Co., New Mexico (Williams, 1978)], in Italy [Tignai quarry in the Susa Valley, Piedmont, (Callegari et al., 2008; Callegari and Boiocchi, 2009) and l'Alpe Cedo, val d'Ossola (Perchiazzi, 1989)], in Austria [Untersulzbach Valley, (Niedermayr et al., 1984), Wurtengebiet, Hohe Tauern (Niedermayr et al., 2001), Wiesbachrinne, Habachtal (Niedermayr et al., 2012)].

Thiobismuthites are also known from the Rudnik polymetallic deposit, in central Serbia (Stojanović et al., 2006). Here they are most abundant in massive sulfide ores (pyrrhotite-colloform-pyrite and/or galena-chalcopyrite mineral parageneses), and to a lesser extent in garnet-epidote-sulfide skarns. Previous research determined three members of thiobismuthites in this polymetallic deposit: cosalite, galenobismutite, and vikingite (Stojanović, 2005). The present study focuses on the new occurrence of aschamalmite within the skarn-replacement and hydrothermal ores from the Rudnik polymetallic deposit. Special emphasis is made on its paragenetic relationships, and the genetic significance of mineral assemblages as indicators of ore formation conditions. Mineralogical, crystallographic, chemical, physical and optical data of aschamalmite are also discussed in detail.

OCCURRENCE AND GEOLOGICAL SETTINGS

Within the Serbo-Macedonian Metallogenic Province (SMMP), which is a part of the Alpine metallogenic unit, ore deposits are hosted in a number of geotectonic units that embrace part of the Vardar ophiolite zone, Serbo-Macedonian massif, and a small part of the Dinarides (Figure 1a). This metallogenic province has been delineated mostly by reference to the Neogene metallogeny and is related predominantly to granodiorite magma. These deposits include the most significant Pb-Zn, Sb, Bi and Mo deposits in Serbia, as well as smaller Cu, Fe, Sn, Ag and minor U, W and Hg deposits (Janković, 1990).

The Šumadija Metallogenic District (ŠMD) belongs to the SMMP. Volcanic/plutonic magmatism with an absolute age of 26.1-31.9 Ma (Cvetković et al., 2004) in the ŠMD was initiated by one of the orogenic phases during the Oligocene, and covers a relatively narrow area (up to 30 km in width) that extends from Belgrade to Kraljevo (Figure 1a). Smaller metallogenic provinces are isolated within several ŠMD orefields. At Avala-Kosmaj the ore deposits consist of hydrothermal Pb-Zn veins (Crveni Breg, Ljuta Strana, Prečice, Babe), and mineralized fractures composed of cinnabar (Šuplja Stena). The Bukulja-Brajevac ore mineralization is related to the Bukulja granitoid and dacite-andesite rocks including pegmatites, cassiterite, and minor wolframite in greisen, hydrothermal uranium veins in granites, and occurrences of Sb. In the Rudnik polymetallic deposit, skarn-hydrothermal Pb-Zn/Cu,Ag,Bi,W associations dominate along with subordinate Sb and Hg (Takovo), and U mineralization (Mandra). Finally, the Kotlenik deposit is characterized by small hydrothermal Pb-Zn veins, and minor U mineralization (Janković, 1990) (Figure 1a).

The area of the Rudnik orefield (ROF) is of oval shape, elongated in a NW-SE direction, and covers approximately 35 km^2 in areal extent. It is mostly primarily composed of sedimentary and secondarily of igneous rocks (Figure 1b). Sedimentary rocks are represented by sandstone, siltstone, limestone (K13,4); marly limestone (K1,2); Upper Cretaceous flysch; and marly limestone (K22,3). The beginning of Oligocene dacite and quartz latite volcanic activity has an absolute age of 30.2 Ma (Cvetković et al., 2004). Vein-like equivalents of granitoid rocks of quartz monzonite and granodiorite composition also occur, but to a lesser extent. Contact-metamorphic rocks are represented by low grade metamorphic marly-clayey sediments, sandstones and conglomerates; hornfels; and Ca-skarns. The origin of these rocks is closely related to the emplacement and crystallization of igneous rocks which provided both the heat for their metamorphism and the differential pressures which created channels for transportation of mineralized hydrothermal solution that impacted alteration of host and country rocks (Ilić, 2000).

The name of the Rudnik Pb-Zn/Cu,Ag,Bi,W polymetallic deposit and mine comes from the Serbian "rudnik"-mine, and is also the name of the mountain Rudnik, in which it is located. The remains of old works indicate that mining activities in this region date from the Neolithic Period and again during the Roman Empire. This polymetallic deposit includes over 90 hydrothermal and skarn-replacement orebody types and is primarily hosted by Cretaceous sediments, occasionally by Oligocene

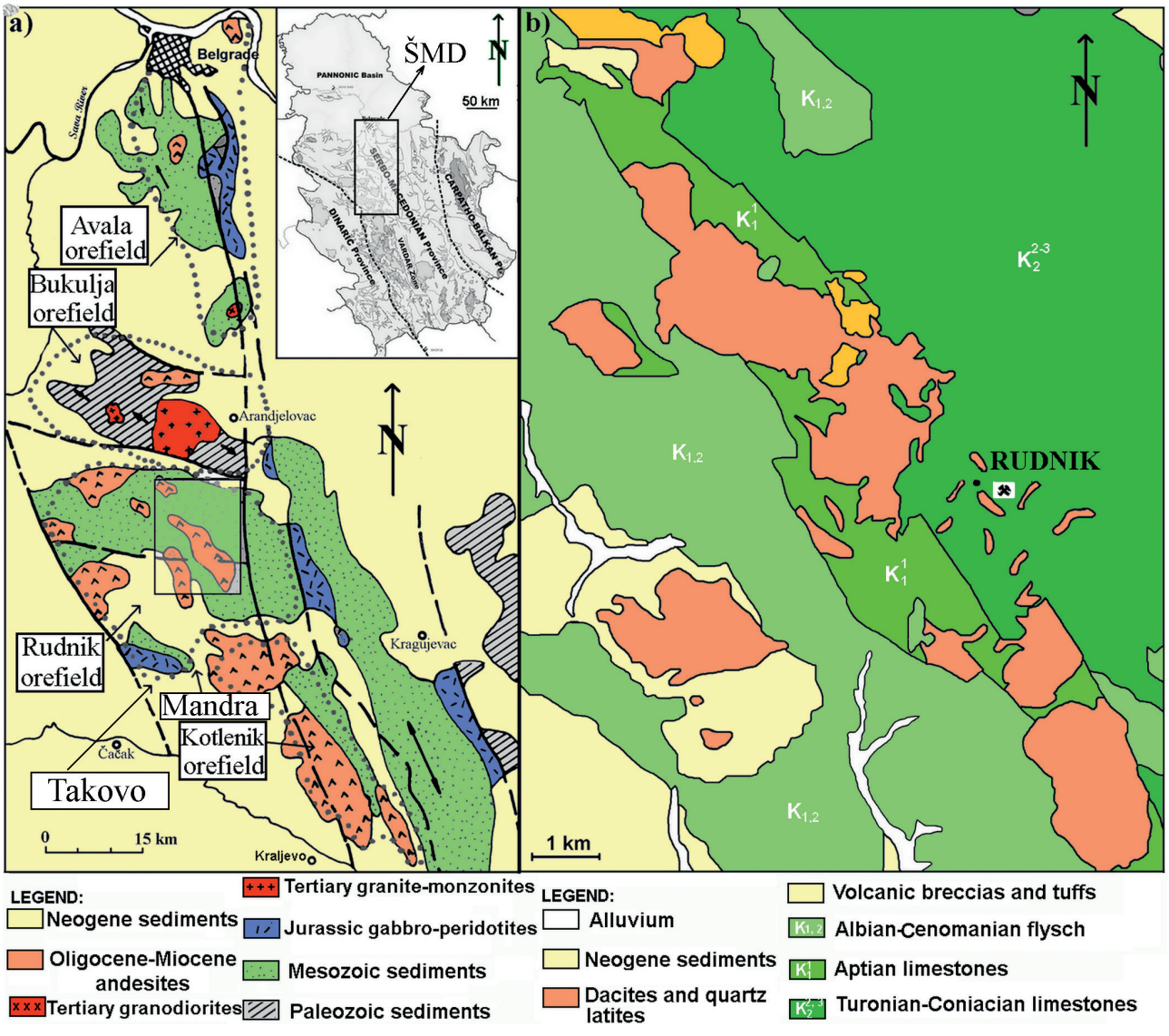

Figure 1. a) Simplified geological map of the Šumadija Metallogenic District (ŠMD) showing the distribution of the orefields (Janković, 1990); b) Geological map of the Rudnik orefield (modified according to the Basic Geological Map of Serbia-1:100,000; sheets L34-137 Gornji Milanovac, and L34-138 Kragujevac).

dykes and sills (dacite, less quartz latite), and contact-metamorphic-metasomatic complex rocks. The most important characteristics of polymetallic mineralization of the Rudnik Pb-Zn/Cu,Ag,Bi,W deposit were reviewed by Rakić (1952; 1958), Milić (1972), and Stojanović et al. (2006).

The orebodies, which are oriented in a NNW-SSE direction, have an areal extent of 6 km^2 (Figure 2). Morphologically, they are of irregular plate- and lens-like shape and are pseudo-layered. The Rudnik polymetallic deposit is divided into several ore zones named after nearby localities. Aschamalmite occurs in the Azna ore zone, located in the northern part of the central area of the deposit (Figure 2). This ore zone is important for its high Cu, Ag, Bi contents and consists of two orebodies (Z1 and Z2) belonging to complex morphogenetic types having massive, brecciated, band-like, and impregnation textures (Figure 2 a,b,c).

The mineralogical composition of the ore is rather complex as more than 70 different species have been identified (Rakić, 1958). Among them are numerous Bi-minerals such as native bismuth, bismuthinite, cosalite, galenobismuthite, and vikingite (Stojanović, 2005); scheelite (Radosavljević et al., 2006; Stojanović et al., 2006); common sulfides such as pyrrhotite, colloform pyrite, chalcopyrite, galena, sphalerite, arsenopyrite and

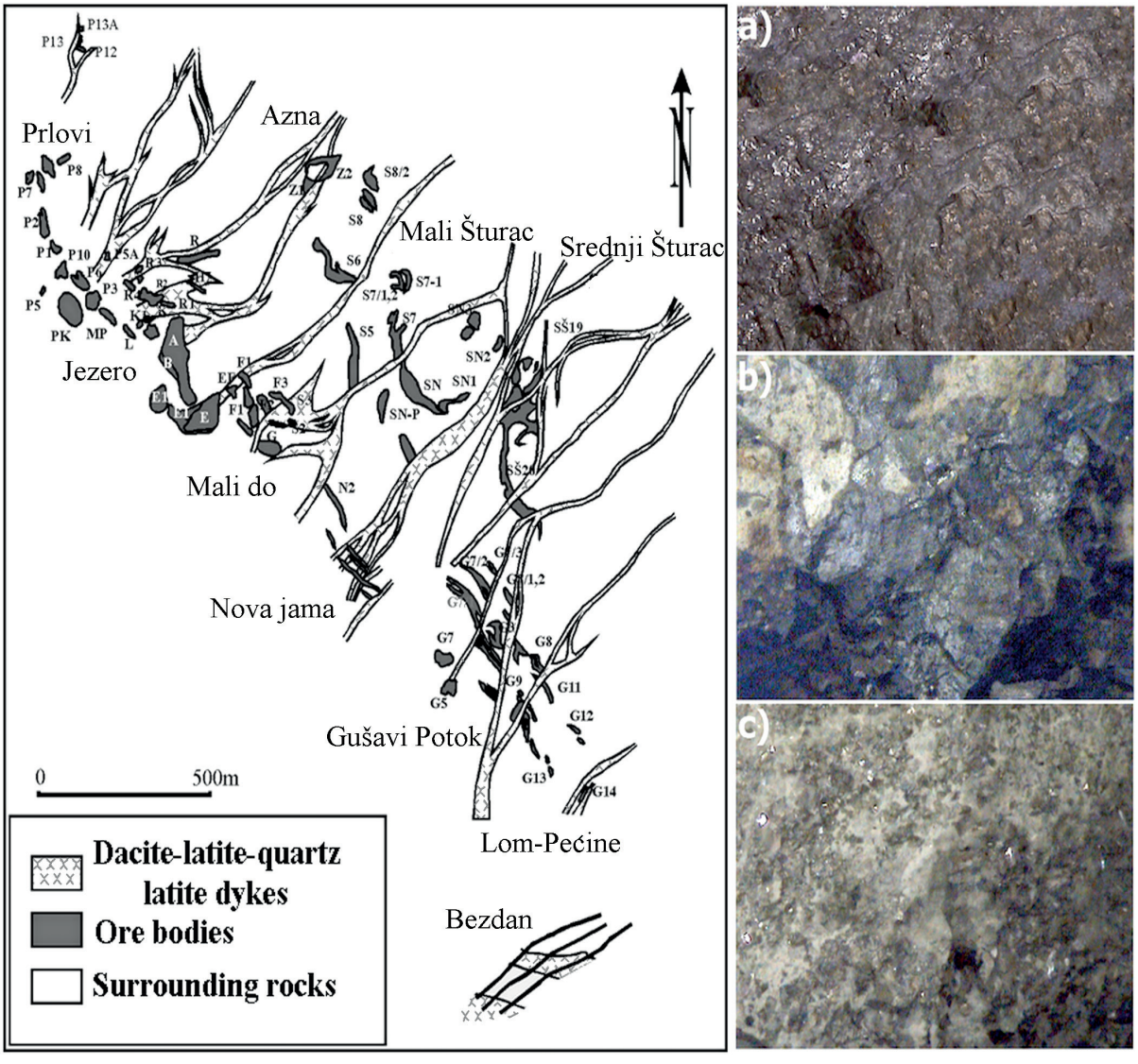

Figure 2. Arrangement of ore zones within the Rudnik deposit (Ilić, 2000). Macroscopic appearance of textural motifs of polymetallic ore from the Azna ore zone: a) massive; b) brecciated; c) impregnation.

other, as well as PGE-minerals (Zarić et al., 1992a), and some nickel sulfides and arsenides (Cvetković, 2001).

MATERIALS AND METHODS

All analyzed samples were collected from horizons 815 (19 polished sections) and 720 (11 polished sections) of the Azna ore zone within the scientific project: "Study of the Rudnik polymetallic deposit from the aspect of gold and platinum group elements (PGE) recovery" (Zarić et al., 1992b). Polished sections were prepared for reflected-light microscopy and electron microprobe analyses (EPMA) by following standard preparation and polishing steps (Picot and Johan, 1982). A Carl-Zeiss polarizing microscope, model Jenapol-U equipped with 10×, 20×, 50×, air medium, 100×, immersion medium objectives and a system for microphotography (Axiocam 105 color camera equipped with Carl Zeiss AxioVision SE64 Rel. 4.9.1. software package) was used for ore microscopic investigations.

The reflectance measurements of aschamalmite were performed in air from 400 to 700 nm using a Vickers M-74 reflectance polarizing microscope equipped with an EMI 9592 B photomultiplier with S-10 response and a SiC-standard Nº 154 supplied by Carl Zeiss, Oberkochen. Four values (470, 546, 589, 650 nm) supplied by the IMA/COM (The Commission on Ore Mineralogy of the International Mineralogical Association) were obtained by interpolation.

Mass spectrometric analyses (MSA) on pure pyrrhotite grains and ore samples were made by a JEOL, model

01MB mass spectrometer with an analytical range of <1000-0.01 ppm. The concentrate of aschamalmite was analyzed by AAS (AAS-Perkin Elmer AA-300). The iron content determined by AAS was used as a standard.

The EPMA were carried out on a JEOL JSM-6610LV scanning electron microscope (SEM) connected with an INCA energy-dispersion X-ray analysis unit (EDX). An acceleration voltage of 20 kV was used for these analyses. The analyzed samples were coated with carbon (density 2.25 g/cm^3) in a15 nm thick layer. For quantitative analyses the following standards were used: FeS_2 (Fe Ka, S Ka), ZnS (Zn Ka, S Ka), Mn (Mn Ka), Ni (Ni Kα), Co (Co Kα), Cu (Cu Ka), InAs (As Ka,), InSb (Sb La), SnO_2 (Sn Lα), Ag_2Te (Ag La), CdS (Cd La), PbS (Pb Ma), and Bi (Bi Ma). This EDX unit has a detection limit of 2σ~0.3 wt%. Crystallochemical formulae were calculated according to Anthony et al. (1990).

In order to find a sample for the single-crystal XRD study, a concentrate of aschamalmite was manually singled out using a stereomicroscope. Unfortunately, numerous attempts to refine the crystal structure of aschamalmite using X-ray diffraction on both a single-crystal and powdered samples were not successful, due to a very low degree of crystallinity, and that no suitable single-crystal was found. However, the XRD powdered sample method was used to determine the unit-cell parameters of aschamalmite from the Rudnik polymetallic deposit. The XRD patterns were obtained on a Philips PW-1710 automated diffractometer using a Cu tube operating at 40 kV and 30 mA. The instrument was equipped with a diffracted beam, curved graphite, monochromator and a Xe-filled proportional counter. The diffraction data were collected in the 2θ Bragg angle range from 5 to 75°, counting for 0.5 s (qualitative identification) and 5 s (calculation of the unit-cell parameters) at every 0.02° step. The divergence and receiving slits were fixed at 1 and 0.1, respectively. All the XRD measurements were performed at room temperature in a stationary sample holder. LSUCRIPC (least square unit cell refinement) software was used for the refinement of the unit-cell parameters (Garvey, 1986).

RESULTS

Chemistry of the ore

Orebodies of the Rudnik polymetallic ore deposit are characterized by complex chemical compositions ranging from Pb-Zn ores with enriched Ag content to Pb-Zn-Cu ores with increased amounts of Bi and W. Compositional changes are manifested over relatively short distance probably due to the rapid and complex changes in evolution of hydrothermal solutions. The ore mass is characterized by wide associations of the main ore metals Pb, Zn, Cu, while Ag, Bi, W, and As occur only locally.

Average contents of ore metals in the Azna ore zone are as follows: Pb=0.94, Zn=0.59, Cu=1.12, WO_3=0.35 wt%; Ag=91, Au=0.3, Bi=90 ppm (Ilić, 2000).

MSA yielded minimum and maximum contents of micro and trace elements in the Azna ore zone (in ppm): B 60->1000, F 80-400, P 330->1000, Cl 70-230, V 70-80, Cr 280-730, Co 145-200, Ni 190->1000, Ga 30-65, As 60->1000, Rb 40-220, Sr 390-570, Y 10-20, Zr 30-250, Nb 4-6, Sn 20-40, Cs 30, Ba 15-160, REEs Σ36.37-67.57 (La 7.54-19.09, Ce 16.28-24.03, Pr 1.98-4.35, Nd 7.81-17.10, Sm 1.16-1.40, Gd 1.60), and Th 0.27-1.40; Sc, Se, Ge, Sr, Mo, In, Te, Eu, Tb, Dy, Ho, Er, Tm, Yb, Lu, Hf and U (qualitatively proven presence); Na, Mg, K, Al, Si, S, Ca, Ti, and Mn are >1000; and Fe 9.91-12.43 wt% (standard) (four analyses).

MSA showed the presence of all rare earth elements (REEs). Among them, La, Ce, Pr, Nd, Sm, and Gd were found in relatively high concentations, while the rest were qualitatively determined. The presence of REEs, however, is not unusual for the Rudnik mine, although their host minerals still have not been determined with certainty, except for monazite-(Ce). High contents of Cr, Co, and Ni in the ore are most likely, remobilized from serpentinite in the ophiolitic zone. The presence of nickel sulfides with cobalt was additionally determined (Cvetković, 2001), while EPMA yielded a content of 0.61 wt% of Cr_2O_3 in epidote.

High contents of Rb, Sr and Ba can be explained by effects of cation substitution in K-feldspars (sanidine, "adularia"). According to Radosavljević et al. (2006), dykes of quartz latite composition are extremely rich in potassium, where K_2O ranges from 6 to 12 wt%, and measured up to a high of 16 wt%. High potassium content is a result of intensive K-metasomatism with adularization. Available radiometric ages indicate the onset of ultrapotassic volcanism around 30 Ma in the northern part of the province along the WNW-ESE trending Zvornik line, where peripheral parts of the ROF are located (Cvetković et al., 2004, Prelević et. al., 2005).

Ore mineralogy

According to the ore microscopic investigation and EPMA, the list of minerals from the Azna ore zone (horizons 815 and 720) are summarized in the Table 1.

Sulfides

Fe-sulfides are characteristic for both 815 and 720 horizons. The most abundant ore minerals in the Azna ore zone are Fe-sulfides (up to 65 mass %), where pyrrhotite, colloform pyrite, marcasite and pyrite dominate. Pyrrhotite commonly occurs in plate-like aggregates, composed of stubby crystals. Although its presence is determined in the surrounding silicate matrix, isolated droplets of native bismuth occur rarely along aggregate boundaries. The cental parts of spherulitic aggregates are composed

Table 1. Mineral composition from the Azna ore zone.

Mineral groups	Minerals
Sulfides, complex sulfides	pyrrhotite, pyrite, marcasite, arsenopyrite, chalcopyrite, Cu-bearing pyrrhotite, cubanite, mackinawite, sphalerite, galena, bismuthinite, argentopentlandite, gersdorffite
Sulfosalts	aschamalmite, galenobismutite
Native metals and alloys	bismuth, silver, PGE
Oxides and tungstates	rutile, anatase, scheelite
Gangue minerals	sanidine, Ca-bearing albite, axinite, hedenbergite, epidote, garnets, clinozoisite, biotite, chlorites, quartz, calcite, siderite, apatite, zircon, monazite-(Ce), anglesite, cerussite, smithsonite, malachite, tenorite, cuprite, Fe-oxy-hydroxides

of pyrrhotite, while peripheral parts are characterized by rhythmic, elliptical, broad, annular zones of colloform relic pyrrhotite (Figure 3a). These aggregates are often cataclased or translationally shifted. Siderite occurs along pyrrhotite-colloform pyrite contacts (Figure 3b). Pyrite is partly a product of hydrothermal transformation of pyrrhotite. Aggregates having "bird's-eye" texture are less affected by alteration processes. MSA of the pyrrhotite concentrate gave the following average contents of micro and trace elements (in ppm): B 35, F 270, Na 160, P 190, Cl 45, K 260, Ti 680, V 7, Cr 215, Mn 470, Co 320, Ga 3, As 550, Rb 4, Y 10, Zr 10, Nb 2, Ag 140, Cd 40, In 1; Sn 1, Sb 9, Te 3, Cs 5, Ba 25, REEs Σ5.56 (La 1.84, Ce 2.83, Pr 0.89), Bi 230.The presence of Mg, Sc, Se, Ge, Sr, Mo, Pr, Nd, Sm, W and Th (proven qualitatively). Al, Si, S, Ca, Ni, Cu, Zn, and Pb are all >1000. The standard contained 56.97 Fe wt%. The atomic ratio of Na/K in the pyrrhotite concentrate is 0.65.

Macroscopically, colloform pyrite occurs in the form of black and yellowish-black spheroids up to 10 mm in diameter that form irregular clusters of kidney-like aggregates. Rhythmic concentric zones cemented with siderite sometimes occur as well (Figure 3 b-c). Red scums composed of Fe-oxy-hydroxides are characteristic for siderite and is due to rapid oxidation. Colloform pyrite is quite an abundant mineral and is frequently cataclased with relic remains embedded in younger sulphides as "isolated islands".

Arsenopyrite is usually related with the arsenization process of parent igneous rocks, although it is less abundant than Fe-sulfides in the Azna ore zone. Arsenopyrite is also deposited along cracks and fissures as crystal druses composed of radially-twinned, euhedral crystals (Figure 3d). Mineralized rocks have brecciated textures as a result of crushing during tectonic processes and later cementation with sulfide-carbonate mineralization, which is typical for the upper parts of orebodies from the horizon 815.

Chalcopyrite either forms as large masses or it occurs as cement to cataclased Fe-sulfides and arsenopyrite. It occassionally forms complex intergrowths with galena overgrowing the siderite matrix. Elongated lath-like crystals of galenobismutite and native bismuth occasionally occur interspersed within large chalcopyrite masses as exsolution products of the high-temperature Bi_2S_3-PbS system (Figure 3e). Sphalerite disease in chalcopyrite is quite common, locally forming dense

Figure 3. Reflected light and SEM-BSE photomicrographs of structural-textural characteristics of ore minerals from the Rudnik polymetallic deposit (Azna ore zone): a) a part of a colloform pyrite overgrown by intensively cataclased pyrrhotite (air, //N); b) preserved forms of relic colloform pyrite (light yellow) cemented with galena (white) and siderite (black) (air, //N); c) macroscopic appearance of a zoned colloform pyrite aggregate with siderite (black) and various sulfides (light) (BEI); d) cataclased crystals of arsenopyrite in silicate matrix (air, //N); e) chalcopyrite with lath-like mix-crystals composed of galenobismutite, and native bismuth (air, //N); f) native bismuth (white) embedded in galena (light gray), and rimmed bismuthinite (gray) (BEI); g) the sphalerite-galena-pyrrhotite mineral paragenesis with inclusion of Cu-bearing pyrrhotite (air, //N); h) a crystal of argentopentlandite (light) with native silver (white) deposited along fissure in pyrrhotite (gray) (BEI); i) an euhedral crystal of native bismuth (white) embedded in galena (white) (BEI); j) a droplet of PGE as an inclusion in pyrrhotite (air, //N); k) euhedral crystals of hedenbergite (dark gray) forming micro-skarn in chalcopyrite (gray) (BEI); l) a mixed aggregate composed of galenobismutite and native bismuth with skeletal crystals of gersdorffite accompanied with scheelite (air, //N); m) an aggregate of aschamalmite with clearly visible effects of bireflectance (air, //N); n) polysynthetic twins of aschamalmite with clearly visible effects of bireflectance (air, //N); o) cataclased parts of aschamalmite with clearly visible effects of bireflectance (air, //N). Mineral abbreviations: Ag=native silver, Agp=argentopentlandite, Am=aschamalmite, Ap=arsenopyrite, Bi=native bismuth, Bt=bismuthinite, Cp=chalcopyrite, Cup=Cu-bearing pyrrhotite, Cs=silicates, Gb=galenobismutite, Gn=galena, Cpy=colloform pyrite, Gz=gersdorffite, PGE=platinum group elements, Po=pyrrhotite, Sch=scheelite, Sid=siderite, Sl=sphalerite.

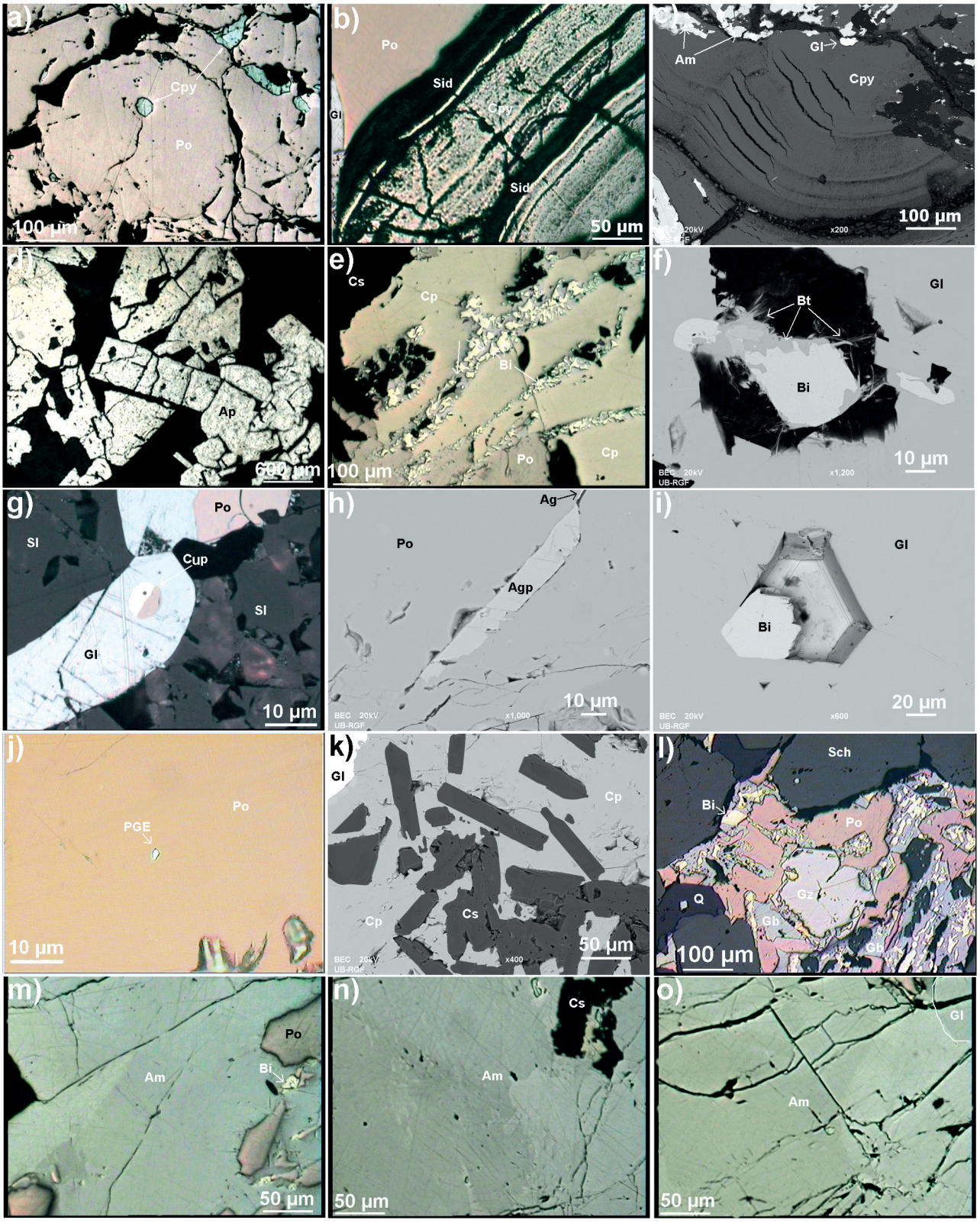
a)
Cpy
Po
100 µm
b)
Po
Sid
Gl
Cpy
Sid
50 µm
c)
Am
Gl
Cpy
100 µm
d)
Ap
600 µm
e)
Cs
Cp
Bi
Po
Cp
100 µm
f)
Gl
Bt
Bi
10 µm
g)
Po
Sl
Cup
Sl
Gl
10 µm
h)
Ag
Po
Agp
10 µm
i)
Gl
Bi
20 µm
j)
Po
PGE
10 µm
k)
Gl
Cp
Cp
Cs
50 µm
l)
Sch
Bi
Po
Q
Gz
Gb
Gb
100 µm
m)
Po
Am
Bi
50 µm
n)
Cs
Am
50 µm
o)
Gl
Am
50 µm

arrays along crystallographic directions. Chalcopyrite additionally displays polysynthetic lamellae having distinct anisotropy, suggesting its crystallization at very high temperatures. Moreover, it frequently occurs as cement in pyrrhotite fissures, torn fragments of ore, and/or it is deposited along pyroxene cleavage planes. According to EPMA it is of typical stoichiometric composition. Chalcopyrite, Bi-minerals and scheelite are characteristically concentrated in the lower parts of the studied orebodies from horizon 720. Mackinawite and cubanite also occur as numerous tiny inclusions of thin lamellae or irregular forms in chalcopyrite, probably representing exsolution from a more compositionally permissive chalcopyrite.

Galena is widespread in the Azna ore zone; however, its relative abudance varies. It occurs as small jagged patches associated with pyrrhotite and silicates. To a lesser extent, galena aggregates are accompanied by wormy pyrrhotite, chalcopyrite, and locally abundant native bismuth as exsolution products of the FeS-PbS-Bi system. Along with native bismuth embedded in galena, younger bismuthinite as needle-like to woolly crystals is common (Figure 3f). Relics of spherulitic Cu-bearing pyrrhotite occur along sphalerite grain boundaries that are extensively overgrown by galena (Figure 3g). EPMA showed that galena frequently contains Ag (up to 0.62 wt%), while Bi and Sb are below detecton limits (<~0.3 wt%).

Sphalerite is less abundant than galena. It occurs in coarse crystalline aggregates (Figure 3g), belonging to the Fe-rich (marmatite) variety. Irregular, band-like intergrowths of pyrrhotite and chalcopyrite sometimes occur in the form of square, hexagonal, and rhombohedral sections that are usually replaced with galena, or intergrown with snowflake-like inclusions of chalcopyrite. EPMA showed that sphalerite contains up to 18.4 mol% FeS, up to 0.30 wt% Mn, and up to 0.52 wt% Cd. Cu, In, Ge, and Sn are below detecton limits of <~0.3 wt%.

Cvetković (2001) determined the presence of Ni-minerals (pentlandite, gersdorffite, and nickeline) 400 m beneath the footwall. They are associated with the nickel-pyrrhotite mineral paragenesis and are deposited within a serpentinite matrix. Moreover, gersdorffite, associated with galena, pyrrhotite, galenobismutite, native bismuth, scheelite, and quartz, has been microscopically determined in the Nova Jama and Azna ore zones (Figure 3l). This study additionally documented the presence of argentopentlandite for the first time in this region, although its occurrence is well-known in numerous localities worldwide (e.g. Groves and Hall, 1978; Augsten et al., 1986; Benvenuti, 1991; Němec and Scharmová, 1992; Barkov et al., 2002; Maier et al., 2008). Argentopentlandite, accompanied by native silver, appears as elongated crystals (90-115 μm in length), filling cracks and fissures in pyrrhotite (Figure 3h). In reflected light, it shows perfect octahedral {111} cleavage. It is optically isotropic, with a pink-brown (in air) and cinnamon-brown (in oil immersion) color, close to bornite, but somewhat lighter. Argentopentlandite has a lower microhardness than that of pentlandite and chalcopyrite. The analytical data for argentopentlandite are summarized in Table 2. The crystallochemical formula of argentopentlandite as determined by 8 spot analyses is $Ag_{1.03}(Fe_{4.81}Ni_{3.14})_{\Sigma 7.95}S_{8.02}$. The Fe/Ni atomic ratio ranges between 1.5 and 1.6 (Table 2).

Bismuthinite is rare as it mostly originated as a reaction product and is found along narrow partings between galena and native bismuth (Figure 3f). It appears along grain boundaries as needle-like, fibrous, and woolly crystalline aggregates overgrowing native bismuth. According to EPMA, it is of typical stoichiometric composition. Ag, Te, and Se are below detection limits of <0.3 wt%.

Native metals

The most abundant native metal is bismuth associated with Pb-Bi sulfosalts, galena, and pyrrhotite. It is commonly of hexagonal and oval shape (Figure 3i), and sometimes occurs as droplets or emulsion inclusions in galena. Crystals of native bismuth mostly occur in contact with pyrrhotite, and rarely with silicates. EPMA yielded silver contents from <0.3 to 0.67 wt%, with oxygen content from 0.5 to 0.7 wt%. Te, Pb, and Sb were below detection limits (<~0.3 wt%).

Native silver occurs within galena and is often of submicron size. It is also occasionally embedded along fissures of pyrrhotite as coatings associated with argentopentlandite (Figure 3h).

Native PGE minerals, determined only microscopically, are extremely rare, and mostly associated with pyrrhotite (Figure 3j). Zarić et al. (1992b) determined the following PGE contents (in ppb) from a pyrrhotite concentrate: Pd 100, Pt 20, and Rh 10 (Σ_{PGE} 130). These minerals have the following microscopic features: high reflectance (R>60 %); white color with tinge of yellow; isotropic; high hardness and relief (> pyrrhotite). They occur in subtraces in concentrates of magnetic (Pd 30, Rh 2 ppb), and nonmagnetic (Pd 10 ppb) heavy minerals. In addition, Cvetković (2001) noticed similar occurrences of PGE minerals in the Ni-pyrrhotite paragenesis deposited in serpentinites at a depth of 400 m beneath the footwall of the deposit.

Tungstates

Rakić (1958) first described scheelite in the Rudnik polymetallic deposit, but only as a rare mineral. Zarić et al. (1992b) later reported scheelite mineralization as much more disseminated within the Nova Jama and Azna ore zones. Scheelite from the Azna ore zone occurs as individual, coarse-grained, euhedral, tabular crystals (up to 30x10 mm) associated with mineralized skarns

Table 2. EPMA of argentopentlandite (1-8) from the Rudnik polymetallic deposit (Azna, in wt%).

Rudnik, Serbia[a]	S	Fe	Ni	Ag	Total	Fe/Ni
1	31.46	32.64	22.34	13.44	99.88	1.5
2	31.59	31.96	22.63	13.52	99.70	1.5
3	31.05	32.64	22.27	13.68	99.64	1.5
4	31.03	32.65	22.81	13.46	99.95	1.5
5	31.17	32.94	22.30	13.30	99.71	1.6
6	30.99	32.40	22.96	13.34	99.69	1.5
7	31.25	32.89	21.91	13.55	99.60	1.6
8	31.31	32.75	22.07	13.45	99.58	1.6
Average	**31.23**	**32.61**	**22.41**	**13.47**	**99.72**	
Apfu	8.02	4.81	3.14	1.03	17	1.5
σ	0.21	0.31	0.36	0.12		
Oktyabr mine, Russia[b]	31.40	34.70	21.30	13.30	100.70	1.7
El Charcón, Spain[c]	31.28	35.20	20.47	13.39	100.85	1.8
Kamilski Dol, Bulgaria[d]	31.36	36.12	20.69	11.90	100.07	1.8
Talnotry, Scotland[b]	31.50	35.60	20.00	12.10	99.80	1.9
Finnish sulfide deposits[e]	31.58	36.78	20.54	10.72	100.00	1.9

Note: [a]this study; [b]Anthony et al., 1990; [c]Morales-Ruano and Hach-Ali, 1996; [d]Kerestedjian, 1997; [e]Vuorelainen and Häkli, 1972. Apfu: atoms per formula unit.

having sulfide-quartz-silicate ore. Exposed surfaces within the orebodies contain enough scheelite to create the "starry night sky" effect when exposed to UV light. Scheelite is grey-white to white, with vitreous to adamantine luster and a white colored streak. Under short wave UV illumination it has an intense light blue color. Microscopically (reflected light), scheelite is dark grey and has relatively high relief. Strong internal reflections are white colored (Figure 3l). Scheelite often contains hexagonal-shaped and oval inclusions of native bismuth and Pb-Bi sulphosalts (Stojanović et al., 2006).

Physical, optical and chemical properties of Ag-bearing aschamalmite

Lead thiobismuthites are mostly disseminated in the massive sulfide ores (pyrrhotite, colloform pyrite, galena, sphalerite, chalcopyrite and siderite mineral paragenesis), and to a lesser extent in axinite-epidote-sulfide skarn. Within the Rudnik mine, four Pb-thiobismuthites have been identified: i) the Nova Jama ore zone - cosalite, galenobismutite, and vikingite (Bi/Pb atomic ratio 1.0-2.0; Stojanović et al., 2005); ii) the Azna ore zone - aschamalmite, galenobismutite (Bi/Pb atomic ratio 0.3-2.0). All of these Pb-thiobismuthites also typically contain silver from 0.44 up to 8.01 wt%.

Irregular aggregates of aschamalmite are generally embedded in pyrrhotite grains and within colloform pyrite matrix, and to a lesser extent in silicates and chalcopyrite. Well-developed aschamalmite crystals have not been observed, only stocky and spindle-like aggregates up to 10 mm in length intergrown with sulfides. They have a blue- tinged, steel gray color similar to galena. No cleavage is observed. Aschamalmite streak is black with metallic luster.

Aschamalmite in polished section occurs in a form of large irregular aggregates (>100 μm) intergrown with pyrrhotite, colloform pyrite, chalcopyrite, galena, arsenopyrite, and native bismuth (Figure 3 m-o). Gangue minerals are represented by carbonates (siderite), quartz and other silicates. Native bismuth occurs only as exsolution within aschamalmite. This implies that the aschamalmite originally had more Ag than it was determined by EPMA. The exsolved Bi could have compensated for the extra Ag present originally in aschamalmite.

In reflected light, aschamalmite has inclined extinction when sections are parallel to the elongation. Moreover, it is optically anisotropic (reddish-brown tinge) with distinct slightly greenish to gray colored bireflectance. The R1 reflectance curve is similar to galena, while the R2 curve is higher. Aschamalmite reflectance measurements are shown in Figure 4. Measurements in the blue-green part of the spectra are in good agreement with those published

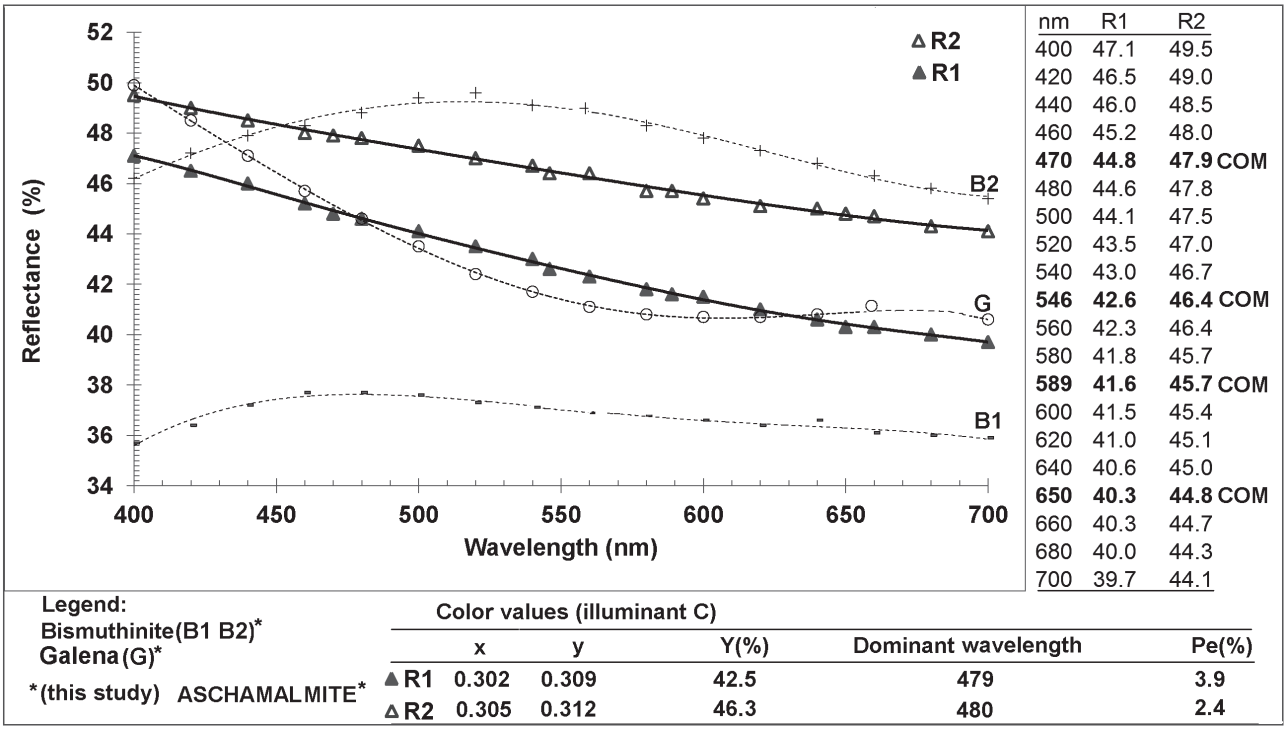

nm	R1	R2	
400	47.1	49.5	
420	46.5	49.0	
440	46.0	48.5	
460	45.2	48.0	
470	**44.8**	**47.9**	**COM**
480	44.6	47.8	
500	44.1	47.5	
520	43.5	47.0	
540	43.0	46.7	
546	**42.6**	**46.4**	**COM**
560	42.3	46.4	
580	41.8	45.7	
589	**41.6**	**45.7**	**COM**
600	41.5	45.4	
620	41.0	45.1	
640	40.6	45.0	
650	**40.3**	**44.8**	**COM**
660	40.3	44.7	
680	40.0	44.3	
700	39.7	44.1	

Legend:
Bismuthinite(B1 B2)*
Galena(G)*
(this study) ASCHAMALMITE

Color values (illuminant C)	x	y	Y(%)	Dominant wavelength	Pe(%)
▲R1	0.302	0.309	42.5	479	3.9
△R2	0.305	0.312	46.3	480	2.4

Figure 4. Results of reflectance measurements and color values of aschamalmite from the Rudnik polymetallic deposit (Azna).

by Mumme et al. (1983), while in the yellow-red part they are slightly lower. This small difference is most probably due to different orientation of measured grains.

The analytical data for aschamalmite are summarized in Table 3. The atomic proportions of each element were calculated to the general formula $Pb_6Bi_2S_9$ that is based on 17 atoms. The crystallochemical formulae of aschamalmite made from an average of six EPMA trials, and from the concentrate of this mineral using AAS amount to $(Pb_{5.82}Ag_{0.20})\Sigma_{6.02}Bi_{2.03}(S_{8.93}Te_{0.02}Se_{0.01})_{\Sigma 8.96}$, and $(Fe_{0.87},Ag_{0.19},Cu_{0.01}Pb_{4.91})_{\Sigma 5.98}(Bi_{1.71},Sb_{0.03})_{\Sigma 1.74}S_{9.27}$, respectively. However, it slightly differs from the EPMA results due to presence of Fe, Sb, and Cu, which likely originate from impurities.

X-RAY POWDER DIFFRACTION (XRD) ANALYSIS OF AG-BEARING ASCHAMALMITE

The $Pb_6Bi_2S_9$ compound also crystallizes in orthorhombic form as heyrovskýite [S.G. Cmcm (63)]. Considerable evidence has accumulated that heyrovskýite can contain appreciable amounts of silver, in the form of the coupled substitution $Ag^{+}+Bi^{3+}=2Pb^{2+}$ (Czamanske and Hall, 1975).

Both aschamalmite and heyrovskýite are members of the lillianite homologue series (heyrovskýite homeotypic series 7L). Aschamalmite crystal structure symmetry is reduced to monoclinic [S.G. *C*2/*m* (12)]. Initially, the unit-cell refinement of aschamalmite was started from the Cmcm space group belonging to heyrovskýite. However, the results were unsatisfactory due to numerous rejected reflections. It was ultimately found that the unit-cell refinement was best calculated in the space group *C*2/*m* belonging to aschamalmite.

The calculated monoclinic unit-cell parameters for aschamalmite are in good agreement with literature data (Callegari and Boiocchi, 2009; Mumme et al., 1983). The Ag-bearing aschamalmite from the Rudnik deposit has slightly increased *a*, decreased *c* and β unit-cell parameters in comparison to Ag-free aschamalmite (Callegari and Boiocchi, 2009; Mumme et al., 1983).

Aschamalmite and heyrovskýite unit-cell parameters, measured from both powder diffraction and single-crystal data, are given in Table 4. Calculated and observed XRD data of aschamalmite from the Rudnik polymetallic deposit obtained by the LSUCRIPC software (Garvey, 1986) are shown in Table 5.

PARAGENETIC SEQUENCE AND CONDITIONS OF THE DEPOSIT FORMATION

The pyrometasomatic (skarn) stage, which is widespread in the Azna and other ore zones in the Rudnik polymetallic deposit, belongs to an axinite-epidote-garnet mineral assemblage associated with other silicates such as hedenbergite (Figure 3k), clinozoisite, etc., and

Table 3. Chemical analyses of aschamalmite (1-7) from the Rudnik polymetallic deposit (Azna ore zone, in wt%).

Rudnik, Serbia[a]	S	Se	Ag	Te	Pb	Bi	Fe	Cu	Sb	Total
1	15.45	0.21	1.09	0.25	62.15	20.82	-	-	-	99.97
2	14.39	-	1.32	-	61.99	22.21	-	-	-	99.91
3	14.20	-	1.07	0.39	62.48	21.91	-	-	-	100.05
4	14.61	-	1.12	-	62.63	21.54	-	-	-	99.90
5	14.93	-	1.03	-	61.59	22.44	-	-	-	99.99
6	14.97	-	1.07	-	61.71	22.08	-	-	-	99.83
Average	14.76	0.04	1.12	0.11	62.09	21.83				99.94
Apfu	8.93	0.01	0.20	0.02	5.82	2.03				17
σ	0.45	0.09	0.10	0.17	0.41	0.58				
7	17.00	-	1.18	-	58.31	20.48	2.79	0.03	0.23	100.02
Ascham Alm, Austria[b]	14.89	(?)	n.d.	(?)	62.95	22.56	-	-	-	100.40
Susa Valley, Italy[c]	14.79	(?)	n.d.	(?)	63.55	21.27	-	-	-	99.61

Note: - <~0.3 wt%; n.d. not detect; (?) no data; apfu atoms per formula unit; 1-6 - EPMA data; 7 - results obtained by AAS; [a]this study; [b]Mumme et al., 1983; [c]Callegari and Boiocchi, 2009.

Table 4. Unit-cell parameters for Ag-bearing and Ag-free aschamalmite and heyrovskýite.

	Composition	*a* (Å)	*b* (Å)	*c* (Å)	*β* (°)	*V* (Å^3)	Space group	Reference
Ag-bearing aschamalmite	$Pb_{5.82}Ag_{0.20}Bi_{2.03}(S_{8.93}Te_{0.02}Se_{0.01})_{\Sigma 8.96}$	13.727(7)	4.122(3)	31.32(2)	90.72(5)	1771.8(1)	*C*2/*m*	This study†
Ag-free aschamalmite	$Pb_6Bi_2S_9$	13.719(1)	4.132(1)	31.419(3)	90.94(1)	1780.8(4)	*C*2/*m*	(1)*
	$Pb_{5.92}Bi_{2.06}S_9$	13.71	4.09	31.43	91.0	1762.13	*C*2/*m*	(2)*
Ag-free heyrovskýite	$(Pb_{5.86}Cd_{0.03})_{\Sigma 5.89}Bi_{2.04}(S_{8.52}Se_{0.53}Cl_{0.03})_{\Sigma 9.08}$	13.7498(4)	31.5053(1)	4.1475(1)	90	1796.66(7)	*Bbmm*	(3)*
Ag-poor heyrovskýite	$Pb_{5.40}Ag_{0.18}Bi_{2.42}S_9$	13.712(2)	31.210 (5)	4.131(1)	90	1767.9(6)	*Bbmm*	(4)*
	$Pb_{5.53}Ag_{0.20}Cu_{0.02}Bi_{2.24}S_9$	13.719	31.260	4.127	90	1769.888	*Bbmm*	(5)†
	$Pb_{5.15}Ag_{0.38}Bi_{2.44}S_9$	13.704	31.247	4.124	90	1765.933	*Bbmm*	(5)†
Ag-rich heyrovskýite	$(Pb_{3.67}Cd_{0.05})_{\Sigma 4.72}Ag_{1.15}Bi_{3.13}S_{9.19}$	4.110(1)	13.600(3)	30.485(12)	90	1704.0(9)	*Cmcm*	(6)*
Synthetic heyrovskýite	$Pb_6Bi_2S_9$	13.719(4)	31.393(9)	4.1319(10)	90	1779.5(1.4)	*Bbmm*	(7)*

Note:(1) Callegari and Boiocchi, 2009; (2) Mumme et al., 1983; (3) Pinto et al., 2011; (4) Takéuchi and Takagi, 1974; (5) Shimizu et al., 1993; (6) Makovicky et al., 1991; (7) Olsen et al., 2011.* Obtained by X-ray single crystal data, † Obtained by powder diffraction data.

Table 5. Comparison of calculated and observed X-ray powder diffraction data of aschamalmite.

I_{rel} (%)	*h k l*	d_{calc}	d_{obs}	I_{rel} (%)	*h k l*	d_{calc}	d_{obs}
39	2 0 $\bar{7}$	3.7696	3.7810	18	5 1 7	2.0262	2.0301
41	2 0 7	3.7264	3.7360	11	6 0 7	2.0265	2.0271
60	1 1 $\bar{4}$	3.5299	3.5411	20	0 0 $\bar{16}$	1.9573	1.9566
56	1 1 4	3.5196	3.5292	14	3 1 $\bar{13}$	1.9012	1.9080
100	2 0 $\bar{8}$	3.4189	3.4292	14	3 1 13	1.8856	1.8881
41	4 0 1	3.4064	3.4051	10	2 2 7	1.8034	1.8000
92	2 0 8	3.3820	3.3914	11	3 1 14	1.7991	1.7955
60	1 1 $\bar{5}$	3.3450	3.3551	11	4 0 $\bar{15}$	1.7938	1.7908
66	1 1 5	3.3341	3.3375	13	5 1 $\bar{11}$	1.7911	1.7884
20	2 0 $\bar{9}$	3.1194	3.1330	11	4 0 15	1.7737	1.7751
28	2 0 9	3.0879	3.1021	28	2 2 $\bar{8}$	1.7650	1.7651
30	3 1 $\bar{2}$	3.0101	3.0077	27	2 2 8	1.7598	1.7581
48	3 1 2	3.0006	3.0000	5	0 0 $\bar{18}$	1.7398	1.7450
86	3 1 $\bar{3}$	2.9452	2.9419	8	2 2 9	1.7141	1.7180
88	3 1 3	2.9318	2.9400	6	8 0 $\bar{3}$	1.6964	1.6991
25	2 0 $\bar{10}$	2.8627	2.8631	7	8 0 3	1.6896	1.6911
64	3 1 $\bar{4}$	2.8601	2.8528	10	2 2 10	1.6670	1.6690
43	3 1 4	2.8437	2.8428	8	4 0 18	1.5439	1.5441
24	2 0 10	2.8356	2.8351	10	6 2 $\bar{6}$	1.4726	1.4750
43	1 1 $\bar{12}$	2.1806	2.1758	10	6 2 6	1.4659	1.4680
38	1 1 12	2.1734	2.1687	9	6 2 $\bar{7}$	1.4524	1.4500
10	5 1 $\bar{5}$	2.1537	2.1478	7	6 2 7	1.4449	1.4441
16	5 1 5	2.1392	2.1390	12	0 2 $\bar{16}$	1.4192	1.4182
19	6 0 $\bar{6}$	2.1050	2.1052	7	3 1 $\bar{20}$	1.3989	1.3962
36	5 1 $\bar{6}$	2.1011	2.0944	7	1 1 21	1.3934	1.3915
33	5 1 6	2.0850	2.0870	7	4 2 $\bar{15}$	1.3530	1.3550
18	6 0 6	2.0856	2.0798	5	9 1 $\bar{8}$	1.3486	1.3472
25	1 1 $\bar{13}$	2.0596	2.0648	8	4 2 15	1.3443	1.3450
64	0 2 0	2.0608	2.0577	8	7 1 15	1.3429	1.3420
18	1 1 13	2.0530	2.0530	8	9 1 8	1.3383	1.3371
16	6 0 $\bar{7}$	2.0473	2.0500	7	9 1 $\bar{10}$	1.3069	1.3090
20	5 1 $\bar{7}$	2.0435	2.0461	5	8 2 3	1.3066	1.0350

pyrite. The presence of small euhedral silicate crystals penetrating older sulfides (Figure 3k) suggests that the skarn stage occurs in two generations, where the younger represents a micro-skarn sub-stage characterized by thermal recrystallization of solid sulfide-silicate melts.

The following mineral parageneses correspond to the high-temperature hydrothermal stage: pyrrhotite-galena-sphalerite-chalcopyrite with Ag and Bi; arsenopyrite-pyrite-galena; colloform pyrite-galena-chalcopyrite-sulfosalts with Ag, Bi, and W; Fe-oxy-hydroxide-Cu-oxy-carbonate. The most significant and of greatest economic importance is the pyrrhotite-galena-sphalerite-chalcopyrite with Ag and Bi phase. This type of mineralization is typically massive, but it is also associated with brecciated mineralization to a lesser extent. The Fe-oxy-hydroxide-Cu-oxy-carbonate mineral paragenesis is thought to have formed during the oxidation processes.

Minerals of the high-temperature pyrrhotite-chalcopyrite-sphalerite-galena paragenesis are low sulfidization (pyrrhotite, marmatite, galena), and were formed in a weak alkaline environment with variable Eh and fS2- conditions (pyrrhotite, colloform pyrite, siderite). The change of pH and Eh conditions, as well as low sulfidization of pre-existing sulfides led to pyrrhotite→marcasite→pyrite hydrothermal alteration (Ramdohr, 1980). Colloform pyrite-galena-chalcopyrite-sulfosalt paragenesis is widespread, occurring throughout the ROF.

Aschamalmite occurs in a specific mineral association with colloform pyrite, pyrrhotite, galena, chalcopyrite, native bismuth, and siderite, and was most probably deposited as a solid of complex composition from high-temperature hydrothermal solutions of the Ag_2S-PbS-Bi_2S_3 system. Mixed aggregates composed of Ag-bearing aschamalmite, Ag-bearing galena and native Bi were formed during cooling. In the Z1 orebody, aschamalmite is apparently exceptionally rare as it was found only in one polished section, occurring as coarse-grained aggregates. Moreover, it has not been determined in any of the other ore zones within the Rudnik polymetallic deposit.

Argentopentlandite is a product of crystallization from high-temperature solutions enriched with silver. It is seen to flow along fissures created in pyrrhotite where Ni and Fe were leached. Due to a lack of open space, and the high hardness of pyrrhotite, argentopentlandite was deposited as elongated crystals filling fissures (Figure 3h). It is invariably an exsolution product in high-temperature Ni- and Ag-bearing chalcopyrite, while a hydrothermal deposition of argentopentlandite is rare, (Mandziuk et al., 1977; Morales-Ruano and Hach-Ali, 1996).

Based on its mineral composition, the Azna ore zone primarily belongs to high-temperature mineral assemblages of low (pyrrhotite, marmatite, Pb-Bi sulfosalts), and high sulfidization (pyrite, arsenopyrite, bismuthinite). As evidenced by aggregates composed of rhythmic, uneven zones of pyrrhotite, pyrite, and siderite, pH and Eh conditions were constantly changing during the period of mineralization. Such mineral associations strongly suggest that the primary hydrothermal solutions containing ore metals were largely complexed with halides (mainly Cl). Moreover, according to the MSA results of polymetallic ores from the Azna ore zone, it is

assumed that the primary hydrothermal solutions during scheelite deposition were acidic and tungsten was also transported in complexes with halides (halide content: 230 ppm F, 130 ppm Cl in polymetallic ore and 700 ppm Cl in pure scheelite, Radosavljević et al., 2006).

Mineral assemblage formation temperatures in the Azna ore zone are difficult to establish, although it is possible to determine the temperature interval. Three different events occurred within this timeframe: i) transformation of chalcopyrite from high to low temperature (400 to 550 °C, according to Craig and Kullerud, 1969); ii) formation of sphalerite "stars" (400 to 500 °C, according to Sugaki et al., 1987), and iii) formation of argentopentlandite (<455 °C, according to Mandziuk and Scott, 1977). Therefore, the most probable formation temperature ranges from 300 to 350 °C.

According to Liu and Chang (1994), aschamalmite is not stable in a PbS-PbSe-Bi_2S_3-Bi_2Se_3 system at 500 °C. This assumption has recently been confirmed by the discovery of heyrovskýite in the fumaroles of Vulcano, Aeolian Islands, Italy, where a temperature close to 500 °C was measured.

Heyrovskýite is also present in deposits formed in a range from 350 to 400 °C (Makovicky et al., 1991). However, aschamalmite crystallizes only at lower temperatures, initially as a partly and then as a completely ordered phase. The rarity of aschamalmite in the lithosphere is probably due to the uncommon P-T conditions required to crystallize a $Pb_6Bi_2S_9$ compound in monoclinic form (Callegari and Boiocchi, 2009).

Excepting Pb-Bi sulfosalts, no other minerals of this group were determined in the Azna ore zone. Arsenic, Sn, and Sb, were all detected, but Hg and Tl are both below detection levels. This suggests that all primary minerals in this ore zone crystallized at high temperatures either as skarn-replacement or from high-temperature hydrothermal solutions. There is additionally a well-developed zonality of medium- to low-temperature mineral associations within the ŠMD (Janković, 1990). Pegmatite-greisen (Bukulja - Sn, W), skarn-replacement, and high-temperature hydrothermal mineralization (Rudnik - Pb-Zn/Cu,Ag,Bi,W, Kosmaj - Pb-Zn/Cu,Sn) are found in the central parts of the ŠMD , while the southern and northern parts of the ŠMD are typified by medium to low temperature hydrothermal mineralizations (Avala - Pb-Zn and Hg; Kotlenik - Pb-Zn).

CONCLUSION

According to microscopic observations and paragenetic analyses, minerals of the Rudnik Pb-Zn/Cu,Ag,Bi,W polymetallic deposit were deposited in several stages, with skarn-replacement and high-temperature hydrothermal stages dominating. Moreover, aschamalmite as investigated belongs to a high-temperature hydrothermal mineral paragenesis, occurring in a specific mineral association accompanied with colloform pyrite, pyrrhotite, galena, chalcopyrite, native bismuth, and siderite. The contents of Pb, Bi and S in the aschamalmite chemical data are in a good agreement with those from published data (Mumme et al., 1983; Callegari and Boiocchi, 2009). However, the key characteristic of aschamalmite from the Rudnik polymetallic deposit is that it contains Ag from 1.03 to 1.32 wt% (Table 3), which is the first such occurrence ever noted. Moreover, apfu (atom per formula unit) of bismuth is >2, while the lack of Pb was complemented with Ag, and is higher than 6. The lack of Sb, Cu and As, and minor contents of Se and Te are also important chemical features. According to optical; XRPD (the unit-cell refinement has best concurrence in the C2/m space group); chemical ($Pb_6Bi_2S_9$ composition with distinct Ag content); and genetic characteristics (crystallization between 300 and 350 °C - skarn-hydrothermal stage) the analyzed mineral was designated with certainty as Ag-bearing aschamalmite. The mode of its crystallization is typical for the high-temperature hydrothermal stage, filling gaps between older sulfides in a form of irregular polycrystalline aggregates.

Besides the ŠMD, rare Pb-Bi sulfosalt mineral parageneses have been identified in the Podrinje Metallogenic District (PMD), Boranja orefield, West Serbia. According to microscopic observations and paragenetic analyses, minerals were formed in several stages with pyrometasomatic (skarn) and high-temperature hydrothermal phases dominating. On the basis of optical, physical, chemical, and crystallographic data, bursaite, cannizzarite, cosalite and aikinite have been determined as Pb-Bi sulfosalts with Cu and Ag (Radosavljević-Mihajlović et al., 2007). In comparison to the other districts within the SMMP (Kopaonik, Rogozna, Golija, etc.), mineral associations of the ROF are distinguished by significant amounts and varieties of Pb-Bi sulfosalts and the unique occurence of Ag-bearing aschamalmite. This study also revealed for the first time the presence of argentopentlandite deposited in the final stage of the high-temperature hydrothermal mineral association.

ACKNOWLEDGMENTS

This paper is a result of a study of the OI-176016 Project (Magmatism and geodynamics of the Balkan Peninsula from Mesozoic to present day: Significance for the formation of metallic and non-metallic mineral deposits), by the Ministry of Education, Science and Technological Development of the Republic of Serbia, which financially supported it. The authors express their deepest gratitude to our colleague Robert Kellie, consulting geologist, for proofreading of the manuscript. Critical reviews of the manuscript by anonymous reviewers led to important modifications of the paper and are highly appreciated. We also acknowledge with thanks the editorial handling of our manuscript by scientific director Antonio Gianfagna.

REFERENCES

Anthony J.W., Bideaux R.A., Bladh K.W., Nichols M.C. (1990) Handbook of Mineralogy. Vol. I. Elements, Sulfides, Sulfosalts. Mineral Data Publishing, Tucson, AZ, USA, 588 pp.

Augsten B., Thorpe I.R., Harris C.D., Fedikow M.A.F. (1986) Ore mineralogy of the Agassiz (MacLellan) gold deposit in the Lynn Lake region, Manitoba. Canadian Mineralogist 24, 369-377.

Barkov A.Y., Laflamme J.H.G., Cabri L.J., Martin R.F. (2002) Platinum-group minerals from the Wellgreen Cu-Ni-PGE deposit, Yukon, Canada. Canadian Mineralogist 40, 651-669.

Benvenuti M. (1991) Ni-sulphides from the Bottino mine (Tuscany, Italy). European Journal of Mineralogy 3, 79-84.

Biruk V.S. and Skakun Z.L. (2000) Bismuth minerals of the Beregovo ore field: minerals assemblages and spatial zonation (Transcarpathian, Ukraine). Geological Quarterly 44, 39-46.

Borodaev Y.S., Garavelli A., Garbarino C., Grillo S.M., Mozgova N.N., Paar W.H., Topa D., Vurro F. (2003) Rare sulfosalts from Vulcano, Aeolian Islands, Italy. V. selenian heyrovskyite. Canadian Mineralogist 41, 429-440.

Callegari A., Boiocchi M., Cech G. (2008) Ritrovamento di aschamalmite in Val di Susa. Micro (notizie mineralogiche) 1, 125-128 (in Italian).

Callegari A.M. and Boiocchi M. (2009) Aschamalmite ($Pb_6Bi_2S_9$): crystal structure and ordering scheme for Pb and Bi atoms. Mineralogical Magazine 73, 83-94.

Chang L.L.Y., Wu D., Knowles C.R. (1988) Phase relations in the system Ag_2S-Cu_2S-PbS-Bi_2S_3. Economic Geology 83, 405-418.

Chutas N.I., Kress V.C., Ghiorso M.S., Sack R.O. (2008) A solution model for high-temperature PbS-$AgSbS_2$-$AgBiS_2$ galena. American Mineralogist 93, 1630-1640.

Ciobanu L.C., Pring A., Cook N.J. (2004) Micron- to nano-scale intergrowths among members of the cuprobismutite series and paděraite: HRTEM and micro analytical evidence. Mineralogical Magazine 68, 279-300.

Craig J.R. (1967) Phase relations and mineral assemblages in the Ag-Bi-Pb-S system. Mineralium Deposita 1, 278-306.

Craig J.R. and Kullerud G. (1969) Phase relations in the Cu-Fe-Ni-S system and their application to magmatic ore deposits. Economic Geology 4, 344-358.

Cvetković Lj. (2001) Ni-Fe mineralization products in the area floor seam deposits of lead and zinc Rudnik mine. Annual of the Yugoslav Association of Mineralogy 3, 135-138 (in Serbian with English abstract).

Cvetković V., Prelević D., Downes H., Jovanović M., Vaselli O. and Pecskay Z. (2004) Origin and geodynamic significance of Tertiary postcollisional basaltic magmatism in Serbia (Central Balkan Peninsula). Lithos 73, 161-186.

Czamanske G.K. and Hall W.E. (1975) The Ag-Bi-Pb-Sb-S-Se-Te mineralogy of the Darwin lead-silver-zinc deposit, southern Califonia. Economic Geology 70, 1092-1110.

Garvey R.G. (1986) LSUCRIPC least square unit-cell refinement with indexing a personal computer. Powder Diffraction 1, 114.

Groves I.D. and Hall R.S. (1978) Argentian pentlandite with parkerite, joseite and the probable Bi-analogue ullmannite from mount Windarra, Western Australia. Canadian Mineralogist 16, 1-7.

Godovikov A.A. (1972) The sulphosalts of bismuth. "Nauka", Moscow, USSR, 247 pp. (in Russian).

Hoda S.N. and Chang L.L.Y. (1975) Phase Relations in the systems PbS-Ag_2S-Sb_2S_3 and PbS-Ag_2S-Bi_2S_3. American Mineralogist 60, 621-633.

Ilić A. (2000) The balance sheet ore reserves of the Rudnik mine (as of 31.12.1999). Technical documentation of the Rudnik mine, Serbia, 84 pp. (in Serbian).

Janković S. (1990) The ore deposits of Serbia: Regional metallogenic settings, environments of deposition, and types. Faculty of Mining and Geology, University of Belgrade, Serbia, 760 pp. (in Serbian with English summary).

Kerestedjian T. (1997) Argentopentlandite $(Fe, Ni)_8$+x$Ag_{1-x}S_8$ from Kamilski Dol a new mineral species for Bulgaria. Bulgarian Geological Society 58, 15-18.

Liu H. and Chang, L.L.Y. (1994) Lead and bismuth chalcogenide system. American Mineralogist 79, 1159-1166.

Maier W.D., Barnes S.J., Chinyepi G., Barton J.M., Eglington B., Setshedi I. (2008) The composition of magmatic Ni-Cu-(PGE) sulfide deposits in the Tati and Selebi-Phikwe belts of eastern Botswana. Mineralium Deposita 43, 37-60.

Makovicky E. (1977) Chemistry and crystallography of the lillianite homologous series. III. Crystal chemistry of lillianite homologues. Related phases. Neues Jahrbuch für Mineralogie Abhandlungen 131, 187-207.

Makovicky E.G. and Karup-Møller S. (1977a) Chemistry and crystallography of the lillianite homologous series. I. General properties and definitions. Neues Jahrbuch für Mineralogie Abhandlungen 130, 264-287.

Makovicky E.G. and Karup-Møller S. (1977b) Chemistry and crystallography of the lillianite homologous series. II. Definition of new minerals: eskimoite, vikingite, ourayite and treasurite. Redefinition of schirmerite and new data on the lillianite-gustavite solid-solution series. Neues Jahrbuch für Mineralogie Abhandlungen 131, 56-82.

Makovicky E., Mumme W.G., Hoskins B.F. (1991) The crystal structure of heyrovskite. Canadian Mineralogist 29, 553-559.

Mandziuk Z.L. and Scott S.D. (1977) Synthesis, stability, and phase relations of argentian pentlandite in the system Ag-Fe-Ni-S. Canadian Mineralogist 15, 349-364.

Milić Č.R. (1972) Metalliferous structure factors control the mineralization area in the polymetallic Rudnik deposit. Proceedings of 7th Congress of Geologists, SFRJ, Zagreb 3, 111-117 (in Serbian with English summary).

Moëlo Y., Makovicky E.G., Mozgova N.N., Jambor L.J., Cook N., Pring A., Paar W., Nickel H.E., Graeser S., Karup-Møller S., Balić-Žunić T., Mumme W.G., Vurro F., Topa D., Bindi L., Bente K., Shimizu M. (2008) Sulfosalt systematics: A review report of the sulfosalt sub-committee of the IMA/COM. European Journal of Mineralogy 20, 7-46.

Morales-Ruano S. and Hach-Ali P.F. (1996) Hydrothermal argentopentlandite at El Charcón, southeastern Spain; mineral chemistry and conditions of formation. Canadian Mineralogist 34, 939-947.

Mozgova N.N. (1985) Nonstoichiometry and a homologous series of sulfosalts. "Nauka", Moscow, USSR, 264 pp. (in Russian)

Mumme W.G., Niedermayr G., Kelly P.R., Paar W.H. (1983) Aschamalmite, Pb5.92Bi2.06S9, from Untersulzbach Valley in Salzburg, Austria-"monoclinic heyrovskyite". Neues Jahrbuch für Mineralogie Monatshefte 10, 433-444.

Němec D. and Scharmová M. (1992) Argentopentlandite in olivine minette near Horní Kožlí, southern Bohemia. Časopis pro mineralogii a geologii 37, 325-328.

Niedermayr G., Postl W., Walter F. (1984) Neue Mineralfunde aus Österreich XXXIII. Carinthia II, 174./94., 243-260 (in Gernan).

Niedermayr, G., Bernhard F., Blass G., Bojar H.P., Brandstätter F., Ettinger K., Graf H.W., Hammer V.M.F., Leikauf B., Meditz H., Moser B., Postl W., Taucher J., Tomazic P. (2001) Neue Mineralfunde aus Österreich L. Carinthia II, 191./111., 141-185 (in German).

Niedermayr G., Auer, C., Bernhard F., Bojar H.P., Brandstätter F., Habel F., Hollerer C.E., Knobloch G., Kolitsch U., Kutil B., Löffler E., Mörtl J., Poeverlein R., Postl W., Prasnik H., Prayer A., Pristacz H., Schachinger T., Steinwender C., Taucher J. Thinschmidt A., Walter F. (2012) Neue Mineralfunde aus Österreich LXI. Carinthia II, 202./122., 123-180 (in German).

Olsen L.A., Friese K., Makovicky E., Balić-Žunić T., Morgenroth W., Grzechnik A. (2011) Pressure induced phase transition in $Pb_6Bi_2S_9$. Physics and Chemistry of Minerals 38, 1-10.

Perchiazzi N. (1989) Aschamalmite: secondo ritrovamento in natura presso l'Alpe Cedo, val d'Ossola Rivista Mineralogica Italiana 4, 238-240 (in Italian).

Picot P. and Johan Z. (1982) Atlas of Ore Minerals. Elsevier, Amsterdam, the Netherlands, 458 pp.

Pinto D., Balić-Žunić T., Garavelli A., Vurro F. (2011) Structure refinement of Ag-free heyrovskyite from Vulcano (Aeolian Islands, Italy). American Mineralogist 96, 1120-1128.

Prelević D., Foley S.F., Romer R.L., Cvetković V., Downes H. (2005) Tertiary ultrapotassic volcanism in Serbia: Constraints on petrogenesis and mantle source characteristics. Journal of Petrology 46, 1443-1487.

Radosavljević S., Stojanović J.,, Radosavljević-Mihajlović A. (2006) Mineralogical and chemical characterization of the W-Pb-Bi-Ag ore from the Rudnik mine, Serbia. Proceedings of TMS 135th Annual Meeting and Exhibition, San Antonio, Texas, USA, 67-71.

Radosavljević-Mihajlović A.S., Stojanović J.N., Dimitrijević R.Ž., Radosavljević S.A. (2007) Rare Pb-Bi sulfosalt mineralization from the Boranja orefield (Podrinje district, Serbia). Neues Jahrbuch für Mineralogie Abhandlungen 184, 217-224.

Rakić S. (1952) Notes on the types of mineralization in the Rudnik mine in Šumadija (Serbia). Glasnik prirodnjačkog muzeja (Bulletin of the Natural History Museum), Series A, 195-203 (in Serbian with German summary).

Rakić S. (1958) A new contribution to knowledge of the mineral assemblages Pb-Zn mine Rudnik in Šumadija, Vesnik (Bulletin), Géologie, Hydrogéologie et Géologie D'Ingénier 14, 233-242 (in Serbian with German summary).

Ramdohr P. (1980) The ore minerals and their intergrowths. Pergamon Press, 1280 pp.

Shimizu M., Kato A., Sakurai K. (1993) Heyrovskýite, lillianite solid solution and galena from the Yakuki mine, Fukushima Prefecture, Japan Resource Geology 43, 283 290.

Stojanović J. (2005) Mineral parageneses of the "Nova Jama" ore zone from the Rudnik polymetallic deposit. MSc thesis, Faculty of Mining and Geology, University of Belgrade, 80 pp. (in Serbian with English summary).

Stojanović J., Radosavljević S., Karanović Lj., Cvetković Lj. (2006) Mineralogy of W-Pb-Bi ores from Rudnik Mt., Serbia. Neues Jahrbuch für Mineralogie Abhandlungen 182, 299-306.

Sugaki A., Kitkoze A., Kolma S. (1987) Bulk compositions of intimate intergrowths of chalcopyrite and sphalerite and their genetic implications. Mineralium Deposita 22, 26-32.

Takéuchi Y. and Takagi J. (1974) The structure of heyrovskýite ($6PbS{\cdot}Bi_2S_3$). Proceedings of the Japan Academy 50, 76-79.

Voudouris P., Spry P.G., Mavrogonatos C., Sakellaris G.A., Bristol S.K., Melfos V., Fornadel A. (2013) Bismuthinite derivatives, lillianite homologues, and bismuth sulfotellurides as indicators of gold mineralization at the Stanos shear-zone related deposit, Chalkidiki, northern Greece. Canadian Mineralogist 51, 119-142.

Vuorelainen Y. and Häkli A.T. (1972) Argentian pentlandite from some Finnish sulfide deposits. American Mineralogist 57, 137-147.

Wang N. (1999) An experimental study of some solid solutions in the system Ag_2S-PbS-Bi_2S_3 at low temperatures. Neues Jahrbuch für Mineralogie Monatshefte 223-240.

Wernick J.H. (1960) Constitution of the AgSbS2-PbS, AgBiS2-PbS and $AgBiS_2$-$AgBiSe_2$ systems. American Mineralogist 45, 591-598.

Williams A.S. (1978) Mineralization at Granite Gap, Hidalgo County, New Mexico. New Mexico Geological Society Guidebook, 29th Field Conference, Land of Cochise, USA, 329-330.

Wu D. (1987) Phase relations in the systems Cu_2S-PbS-Bi_2S_3 and Ag_2S-PbS-Bi_2S_3 and their mineral assemblages. Chinese Journal of Geochemistry 6, 225-233.

Zarić P., Radosavljević S., Jeknić M. (1992a) The preliminary results of the presence of PGE-minerals in the polymetallic deposit Rudnik. Proceedings of 24th International October Conference on Mining and Metallurgy, Donji Milanovac, Serbia, 76-78 (in Serbian with English summary).

Zarić P., Radosavljević S., Janković S., Branković A., Milosavljević B. (1992b) Study of the Rudnik polymetallic deposit from the aspects of gold and platinum group elements (PGE) recovery. Faculty of Mining and Geology, University of Belgrade, 62 pp. (in Serbian).